Digital Signal Processing 38 (2015) 43–52

Contents lists available at ScienceDirect

Digital Signal Processing

www.elsevier.com/locate/dsp

An accurate finger vein based verification system

Puneet Gupta *, Phalguni Gupta

Computer Science and Engineering Department, Indian Institute of Technology Kanpur, Kanpur 208016, India

ARTICLE INFO

Article history:
Available online 16 December 2014

Keywords:
Biometrics
Vein extraction
Variational approach
Vein matching
Multi-scale matched filtering

ABSTRACT

This paper makes use of finger vein to propose an accurate personal authentication system. A matched filtering at various scales is applied on the vein image to reduce the effects of noise occurred due to non-uniform illumination, low local contrast, hairs and skin texture. Vein image is also enhanced by using global characteristics. Local and global characteristics of enhanced vein images are fused to obtain accurate vein pattern. Extracted veins are used for matching such that the problem of geometric deformations can be handled efficiently. For performance evaluation, a publicly available database of 3132 unconstrained finger vein images acquired from 156 subjects is used. Performance of the proposed system is found to be better than the various existing systems.

1. Introduction

The finger vein pattern is the complex structure of superficial blood vessels on the finger. It obeys necessary biometric properties like uniqueness, universality and permanence which makes it useful for personal authentication. Further, it (i) assures liveness; (ii) is contact-less, hence hygienic; (iii) is hard to forge as it lies inside the skin; (iv) is difficult to spoof; and (v) has low failure to enroll and (vi) is highly reliable for personal authentication. Due to these features, vein pattern is regarded as one of the most promising and attracting biometric traits. However, there are various issues which restrict its usefulness. Some of these are (i) skin properties (like pigmentation, thickness and hairs); (ii) environmental conditions (like temperature and visible light interference); (iii) vein patterns have varying widths; (iv) areas captured near interphalangeal joints has high illumination; and (v) finger pose [1].

Like any other biometric system, a finger vein based authentication system mainly consists of five stages and they are data acquisition, region of interest (ROI) extraction, enhancement, vein extraction and feature matching. ROI can be extracted by some morphological operations along with the knowledge of the background and acquisition device. In [2], location of interphalangeal joints has been used for detecting finger area. In the enhancement stage, various operations on finger area are performed such that vein structure is enhanced while noise is suppressed. In addition, problems of non-uniform illumination and low local contrast, are minimized at this stage. Veins are extracted from the enhanced image. Eventually, suitable features from the veins are extracted and matched at the feature matching stage.

Various filters and transforms based on local neighborhoods, such as Gabor filter [3], Steerable filter [2] and Curvelets transform [4] can be used for the vein enhancement. But it is difficult to define a shape for variable width veins. In addition, noise present in a vein closely resembles the vein structure and thus it also gets enhanced. In [5], the local dark position has been used to track the vein structure. It has been modified in [6] by including the maximum curvature information during vein tracking. The intuition behind the usage of vein tracking for vein enhancement is that the vein area can be tracked large number of times from various locations while isolated noise areas are tracked less number of times. But it is observed that thin veins are not tracked quite often due to small width; thus, thin veins are not effectively enhanced. Further, vein tracking neglects the local shape of a vein which can sometime generate spurious veins. In [7] and [8], finger vein images have been enhanced by using restoration algorithms which can minimize the scattering effect generated during IR image acquisition.

Vein is extracted from the enhanced vein image by either global or local adaptive thresholding algorithms. Global thresholding algorithms perform poorly for finger vein images because of the existence of significant overlap between the pixel intensities of foreground and background pixels. In contrast, local adaptive thresholding algorithms perform better for non-uniform illumination and low contrast vein images. But local adaptive thresholding algorithms have the following limitations: (i) they require some tunable parameters; (ii) they do not preserve the vein structure; and (iii) they do not consider the global smoothness criteria. They are highly affected by the suitable selection of neighborhood size.

* Corresponding author.
E-mail addresses: puneet@cse.iitk.ac.in (P. Gupta), pg@cse.iitk.ac.in (P. Gupta).

http://dx.doi.org/10.1016/j.dsp.2014.12.003
1051-2004/

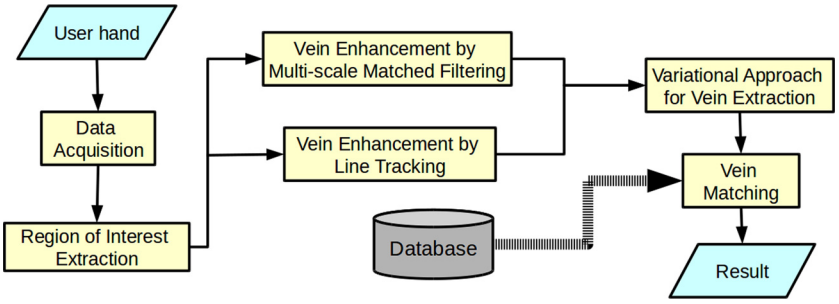

Fig. 1. Flow-graph of the proposed system.

If the size is small then noise cannot be properly suppressed. On the other hand, if the size is large then local details are lost. All these factors generate spurious vein pattern.

Generally, vein matching is accomplished by using features such as minutiae [9], local line binary pattern [10], SIFT [11], soft biometrics [12], statistical measures [13], machine learning [14], correlation (or template) based methods [3] and hybrid algorithms [15]. Use of minutiae for vein matching usually shows poor performance for low quality finger vein images which contain many spurious and few genuine minutiae. Similarly, less number of accurate and distinctive SIFT key-points can degrade the performance of vein matching. Due to finger pose variations, employing a soft biometric trait like the width of phalangeal joint [12] or finger geometry [16] is also not of much use for matching. Use of features extracted by statistical measures (like local moments) for vein matching is ineffective because such statistical features are less discriminating. Also, vein matching through machine learning techniques requires huge amount of training data that can capture most of possible deformations, but it is not always possible [14]. Correlation or template based matching gives accurate results even when some genuine veins are missed or spurious veins are introduced. It eliminates rigid deformation through image registration and thus, can also be referred as matching based on rigid registration. Registered images are used to calculate the similarity score. Features used for registration are like vein structure [3] and vein skeleton [17]. But finger poses [18] can deteriorate the performance of correlation or template based matching. In hybrid algorithms, vein matching is accomplished by various ways and there matching scores are later fused. In [15], local features based on local binary pattern are fused with global features based on wavelet by using a machine learning approach. In some algorithms, enhanced vein image is directly used for vein matching without undergoing vein extraction. In [19], enhanced vein image is encoded by using radon transform and matched by the neural network. Similarly, in [20], enhanced vein image is matched by using phase only correlation. Also, texture (by using compcode) of the enhanced vein image is used for feature encoding in [21]. Algorithms which do not use vein extraction give accurate results if finger veins are acquired under controlled environment. But these can be affected by the problems of noise, non-uniform illumination, low local contrast and pose variations.

This paper proposes a finger vein based authentication system which can handle the above issues. It consists of five sections which are region of interest extraction, vein enhancement by multi-scale matched filtering, vein extraction by line tracking, variational approach for vein extraction and vein matching. The flow-graph of the proposed authentication system is shown in Fig. 1. In Section 2, process of ROI extraction from a finger vein image has been presented. Local characteristics of a vein pattern have been used to enhance finger veins. This process has been discussed in Section 3. Next section presents another process which is used to enhance the finger veins by using global characteristics of vein pattern. Fusion of these two enhanced finger vein has been presented in Section 5. Section 6 discusses the matching strategy which can effectively handle the effect of finger poses. Section 7 analyzed the experimental results. Conclusions are given in the last section.

Algorithm 1 *Region_of_Interest_Extraction*(I_V).

Require: Vein image, I_V.
Ensure: Return ROI image containing finger area, B.
1: Remove borders from I_V
2: $I_{boundary} = CannyEdgeDetector(I_V)$
3: $I_{Th} = GlobalThresholding(I_V)$
4: Use $I_{Th}(x, y) = I_{Th}(x, y)(\text{AND}(\text{NOT}(I_{boundary}(x, y))))$ at each pixel (x, y) to remove the boundary from I_{Th}.
5: Extract all components from I_{Th} by using 8-neighborhood connectivity algorithm.
6: Remove small size components.
7: Except remaining component pixels, set all other pixels as background pixels.
8: $B = I_V$
9: $B(\text{background pixels}) = 255$ // setting background pixels to 255
10: **return** B

2. Region of interest extraction

In the vein image, borders of image contain noise and do not provide much vein information because of less exposure to IR light. So, borders of the image can be pruned. Global thresholding algorithm [22] is applied on the pruned image to obtain a binary image where 1 represents the foreground pixels (or pixels belonging to finger). But the pruned image contains noisy background, with high intensity values and large variation in the local neighborhoods. As a result, several background pixels may be wrongly classified as foreground pixels in the binary image. Such a problem of wrong classification mainly occurs near the finger boundary. In the vein images, finger boundaries are clearly defined. Further, boundaries are dilated by using morphological operations. These dilated boundaries are removed from the binary image to remove most of the wrongly classified pixels. Some wrongly classified pixels may still exist in the binary image. 8-neighborhood connectivity algorithm is applied to remove small sized connected components [23]. In addition, remaining components may contain holes which are removed by using morphological operations [24]. ROI is generated by setting all background pixels in the pruned image to 255. Steps used to extract ROI from a vein image is given in Algorithm 1. In addition, an example of ROI extraction is shown in Fig. 2.

3. Vein enhancement by multi-scale matched filtering

The cross section of vein pattern has approximately the Gaussian shape and vein has a line shaped structure. Thus, following filter, G_ϕ, proposed in [25] has been used to extract the vein pattern

$$G_\phi(x, y) = -e^{-\left(\frac{p^2}{\sigma_x^2}\right)} \tag{1}$$

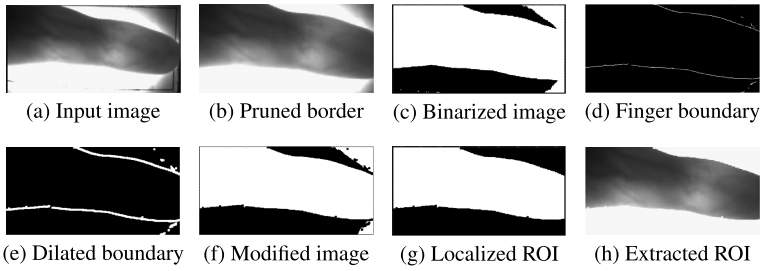

Fig. 2. Various stages of ROI extraction.

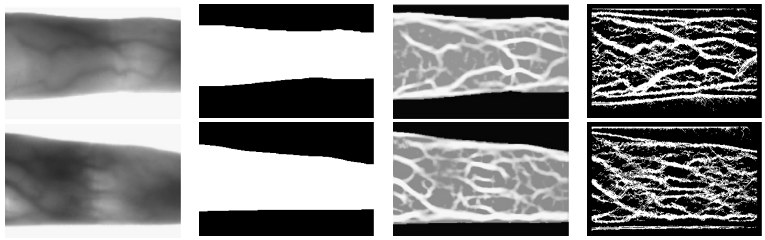

Fig. 3. Various stages of vein enhancement.

where $G_\phi(x, y)$ represents the value of the filter G_ϕ at the pixel (x, y); σ and ϕ are standard deviation and direction respectively; and p is obtained by

$$p = x\cos\phi + y\sin\phi \quad \text{and} \quad |p| \leq 3\sigma_x$$

satisfying $|q| \leq l/2$ where

$$q = y\cos\phi - x\sin\phi$$

and l represents the length in y-direction. Thus, the domain of x and y which depends on p and q are restricted by σ_x and l. Filter, G_ϕ is normalized in such a way that it has zero mean. It can be done by

$$G_\phi(x, y) = G_\phi(x, y) - mean(G_\phi) \tag{2}$$

To extract variable width veins, the filter G_ϕ is applied at multiple scales [26]. Let s represent such a scale at which the proposed filter is required. Then, Eq. (1) is modified as

$$G_{\phi,s}(x, y) = -e^{-(\frac{p^2}{s\sigma_x^2})} - m_s \tag{3}$$

where m_s denotes the mean of the $(-e^{-(\frac{p^2}{s\sigma_x^2})})$ and p is given by:

$$p = x\cos\phi + y\sin\phi \quad \text{and} \quad |p| \leq 3s\sigma_x$$

such that $|q| \leq sl/2$, where

$$q = y\cos\phi - x\sin\phi$$

The filter response of original signal at scale s is given by

$$R_g^s(x, y) = G_{\phi,s}(x, y) \otimes B(x, y)$$

where $\otimes$ and B represent the convolution operator and ROI image. Multi-scale matched filter response, M, is obtained by element-wise product of filter responses evaluated at different scales. That is,

$$M(x, y) = R_g^{s_1}(x, y) * R_g^{s_2}(x, y)$$

Algorithm 2 *Vein_Enhancement*(B, G_1, G_2).

Require: Finger vein ROI image, B, along with filters G_1 and G_2 at different scales.
Ensure: Return vein enhanced image, M.
1: $R_g^{s_1} = G_1 \otimes I_I^R$ // $\otimes$ is the convolution filter
2: $R_g^{s_2} = G_2 \otimes I_I^R$ // $R_g^{s_1}$ and $R_g^{s_2}$ are filter responses
3: $M = (R_g^{s_1} * R_g^{s_2})$ // Pixelwise multiplication
4: **return** M

where $*$ represents element-wise product. M contains spurious veins near the finger boundary which are removed by using finger boundary and morphological operations. Fig. 3(c) illustrates M. It has a brighter intensity near vein as compared to its neighbor and a wide vein has brighter intensity patterns as compared to thin veins. Steps involved for vein enhancement are given in Algorithm 2.

It has been observed that vein pattern is preserved in local neighborhood, even if the vein image contains non-uniform illumination and low local contrast. Therefore, the proposed local vein shape matching effectively enhances the finger veins, regardless of the presence of non-uniform illumination and low local contrast. In addition, variable width veins are enhanced because filtering is carried out at the multiple scales. That is, thin and thick veins can be enhanced at low and high scales respectively, which are eventually consolidated. But sometime noise generated due to hair and texture are also enhanced by the matched filter because it closely resembles the vein structure.

4. Vein enhancement by line tracking

Initially veins are extracted from the ROI by the system proposed in [5]. It uses the intuition that cross section of vein pattern has a valley shape while in orthogonal direction it has a line shaped. Due to valley, local minima can be easily detected in a cross section profile even in the cases of non-uniform illumination. Thus, one can start at a point and track the next point by checking the closest local maxima. Since a vein looks like a line when considered in a small neighborhood, the direction of the next tracking point is restricted. Such a line tracking guarantees that vein areas can be tracked large number of times while spurious areas are tracked only a few times. For initialization, various starting points are selected randomly. Tracking is stopped when there is no lo-

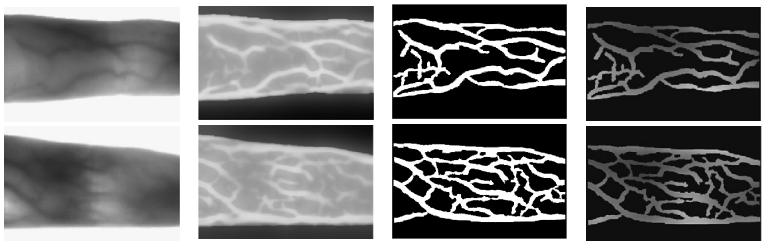

(a) Extracted ROI (b) Threshold surface, T (c) Extracted vein pattern, M (d) Template, I_M

Fig. 4. Output from vein extraction corresponding to Fig. 3.

cal minima to go forward. Eventually, an image is obtained where each pixel stores the number of times it is tracked. It is normalized between 0 and 1 and let it be L. An example of such images is given in Fig. 3(d). It contains high values for vein areas while low values for background areas. Reason behind this is that vein areas can be tracked or reached from various other vein points, but tracking involving a background pixel can be instantaneously stopped due to non-availability of local minima. Since a vein pixel is determined by using the various tracks originated from various randomly selected pixels, vein enhancement using line tracking is regarded as a global vein enhancement algorithm. But such a vein enhancement algorithm has following disadvantages:

1. Accurate local maxima detection is its key requirement which may not be determined due to noise, low local contrast and non-uniform illumination.
2. It assumes that vein areas can be tracked from multiple locations which are usually valid for thick vein. But it fails in the case of thin veins because these are tracked from few locations due to small width [27].
3. It does not consider the shape of the cross sectional vein profile due to which non-vein pixels may also be regarded as vein pixels [6].

5. Variational approach for vein extraction

This section discusses the fusion strategy to fuse vein enhanced images obtained from multi-scale matched filtering and line tracking for vein extraction. Proposed system iteratively determines the threshold surface, T. Examples of T are shown in Fig. 4(d). It does not require any tunable parameter like neighborhood size. Due to this, the proposed system can extract the variable width veins. Observation used to formulate the proposed system is that vein pattern information present in the vein image obtained through multi-scale matched filtering, M, is obtained through vein shape while in other case, vein pattern information obtained by line tracking, L is extracted by the local maxima in a neighborhood. These complimentary informations can be fused for accurate vein extraction. Further, vein extraction by thresholding requires that T should be lesser than M at the vein pixels, while greater than M at background pixels for accurate vein localization. Therefore, T should intersect the image surface at the high gradient location. In addition, a constraint on data fidelity should be maintained by minimizing the similarity between M and T. Similarity between M and T is measured by the sum of squared error and let, it be represented by $F(T)$ which is given by

$$F(T) = \int_x \int_y \big(M(x,y) - T(x,y)\big)^2 \mathrm{d}x\,\mathrm{d}y \tag{4}$$

where (x, y) represents a pixel location. Minimization of $F(T)$ tries to fit the threshold surface as close as possible to M by giving equal weights to each pixel. But T should be accurately modeled near vein pixels. Thus, vein pixels should be given higher weights. To leverage this, a weight parameter is introduced in $F(T)$ by using the vein information given by L. That is, we need to minimize the modified functional given by

$$\hat{F}(T) = \int_x \int_y L(x,y)\big(M(x,y) - T(x,y)\big)^2 \mathrm{d}x\,\mathrm{d}y \tag{5}$$

Such a fusion of vein information in M and L helps in obtaining accurate estimates of T. $\hat{F}(T)$ is minimized if T is equal to M at the places belonging to veins (high value of L) but such a T is highly discontinuous. But in our case T should be less than M at the vein areas for accurate vein extraction. Thus, there is a constraint in $\hat{F}(T)$ which regularizes T and is added. It is minimized along with $\hat{F}$ to obtain the best estimate of T. It is defined as

$$G(T) = \int_x \int_y \big|\bigtriangledown T(x,y)\big|^2 \mathrm{d}x\,\mathrm{d}y \tag{6}$$

where

$$\bigtriangledown T(x,y) = \frac{\partial T(x,y)}{\partial x} + \frac{\partial T(x,y)}{\partial y} \tag{7}$$

It can be observed that $\hat{F}(T)$ and $G(T)$ are competitive. That is, $\hat{F}(T)$ is minimized if M and T are pixel-wise equal at vein pixels, but it requires high value for $G(T)$ near vein pixels. Similarly, $G(T)$ is minimized if T is constant at each pixel which results in high value of $\hat{F}(T)$. To minimize $\hat{F}(T)$ and $G(T)$ simultaneously, these are combined with the help of an adaptive weight parameter, α, which controls the contribution of $\hat{F}(T)$ and $G(T)$. Then, we have

$$P(T,\alpha) = \frac{1}{2}\big(\sqrt{1-\alpha^2}\hat{F}(T) + \alpha G(T)\big) \tag{8}$$

which has concave-convex nature. It is a strictly concave with respect to α while strictly convex with respect to T [28]. One can observe that if $\hat{F}$ dominates over G in P then T is highly discontinuous and results in missing of genuine veins. On the other hand, if G dominates over $\hat{F}$ then T is smooth which can result in the generation of false veins. Hence, T is appropriately obtained by a minimax solution of P. In other words, $P(T,\alpha)$ needs to be minimized in terms of T and maximized in terms of α, that is,

$$\hat{T} = \arg\max_{\alpha} \min_{T} P(T,\alpha) \tag{9}$$

where $\hat{T}$ is the estimated T. Since T and α are compact sets and $P(T,\alpha)$ has concave-convex behavior, $P(T,\alpha)$ has a saddle points which allows the interchange of inner and outer optimizations in a minimax problem [29]. Hence

$$\hat{T} = \arg\min_{T} \max_{\alpha} P(T,\alpha) \tag{10}$$

Solution of this minimax optimization problem can be given by variational minimax optimization.

Algorithm 3 *Vein_Extraction*(B, M).

Require: Vein image B and vein enhanced image M
Ensure: Return I_M which depict the veins
// Extraction of veins from B
L = VeinExtractionByMiuraAlgorithm(B)
L = Normalized(L)
// Initialization
$\bar{\alpha} = 0$
th = OtsuThresholding(M)
Create thresholding surface, T, by putting th at each pixel.
// Iterative update
for $t = 1$ to 100 **do**
  $\alpha_1 = \bar{\alpha}$
  $\hat{F}(T) = \int_x \int_y L(x,y)(M(x,y) - T(x,y))^2 \mathrm{d}x\,\mathrm{d}y$
  $G(T) = G(T) = \int_x \int_y |\frac{\partial T(x,y)}{\partial x} + \frac{\partial T(x,y)}{\partial y}|^2 \mathrm{d}x\,\mathrm{d}y$
  $\bar{\alpha} = \frac{G(T)}{\sqrt{(\hat{F}(T))^2 + (G(T))^2}}$
  At each pixel (i, j), evaluate $T_{i,j}^{new} = T_{i,j} + \tau\sqrt{1-\bar{\alpha}^2}(L_{i,j}(M_{i,j} - T_{i,j})) + \tau\bar{\alpha}(T_{i+1,j} + T_{i-1,j} + T_{i,j+1} + T_{i,j-1} - 4T_{i,j})$
  $T = T^{new}$
  if $\alpha_1 - \bar{\alpha} < \epsilon$ **then**
    break *// This will break FOR loop*
  end if
end for
// Extracting veins from M by using T
For each pixel (x, y), $V_l(x, y) = 1$ if $M(x.y) > T(x, y)$ otherwise $V_l(x, y) = 0$
$I_M = M * V_l$ *// where $*$ is the multiplication operations at all pixels*
return I_M

Initially, Otsu thresholding is applied on B and it is used to form T which is iteratively updated by using Algorithm 3. In its first iteration, $P(T, \alpha)$ is maximized and then minimized with respect to α and T respectively. $P(T, \alpha)$ is first differentiated with respect to α and equate to zero to estimate the value of α which maximizes $P(T, \alpha)$. That is,

$$\frac{\partial P(T,\alpha)}{\partial \alpha} = \frac{-\alpha}{\sqrt{1-\alpha^2}}\hat{F}(T) + G(T) = 0 \tag{11}$$

Let the estimated value of α be $\bar{\alpha}$ which is given by

$$\bar{\alpha} = \frac{G(T)}{\sqrt{(\hat{F}(T))^2 + (G(T))^2}} \tag{12}$$

Then, function $P(T, \bar{\alpha})$ is minimized by using gradient descent to estimate T instead of $P(T, \alpha)$, which is given by

$$P(T, \bar{\alpha}) = \int_x \int_y \Psi(T, T_x, T_y)\mathrm{d}x\,\mathrm{d}y \tag{13}$$

where $\Psi(T, T_x, T_y)$ is given by

$$\Psi(T, T_x, T_y) = \sqrt{1-\bar{\alpha}^2}\big(L(x,y)\big(M(x,y) - T(x,y)\big)^2\big) + \bar{\alpha}\big(\big|T_x(x,y) + T_y(x,y)\big|^2\big) \tag{14}$$

$$T_x(x,y) = \frac{\partial T(x,y)}{\partial x} \tag{15}$$

$$T_y(x,y) = \frac{\partial T(x,y)}{\partial y} \tag{16}$$

Let us assume that there is an arbitrary function, $h(x, y)$, which has continuous first and second derivatives in the image domain. It is used to perturb the threshold surface T. This transforms the initial function $P(T, \bar{\alpha})$ into another function $P(T + h, \bar{\alpha})$. By using Euler conditions, variations introduced in $P(T, \bar{\alpha})$ due to h is given by

$$\delta\big(P(T,\bar{\alpha})\big) = \int_x \int_y \left(\frac{\partial \Psi}{\partial T} + \frac{\partial}{\partial x}\left(\frac{\partial \Psi}{\partial T_x}\right) + \frac{\partial}{\partial y}\left(\frac{\partial \Psi}{\partial T_y}\right)\right) h(x,y)\mathrm{d}x\,\mathrm{d}y \tag{17}$$

where

$$\frac{\partial \Psi}{\partial T} = -\sqrt{1-\bar{\alpha}^2}\big(L(x,y)\big(M(x,y) - T(x,y)\big)\big) \tag{18}$$

$$\frac{\partial}{\partial x}\left(\frac{\partial \Psi}{\partial T_x}\right) = \frac{\partial}{\partial x}\left(\bar{\alpha}\frac{\partial T}{\partial x}\right) = \bar{\alpha}\frac{\partial^2 T}{\partial x^2} \tag{19}$$

$$\frac{\partial}{\partial y}\left(\frac{\partial \Psi}{\partial T_y}\right) = \frac{\partial}{\partial y}\left(\bar{\alpha}\frac{\partial T}{\partial y}\right) = \bar{\alpha}\frac{\partial^2 T}{\partial y^2} \tag{20}$$

For simplicity, assume

$$E_{var} = \frac{\partial \Psi}{\partial T} + \frac{\partial}{\partial x}\left(\frac{\partial \Psi}{\partial T_x}\right) + \frac{\partial}{\partial y}\left(\frac{\partial \Psi}{\partial T_y}\right) \tag{21}$$

Change in T obtained by the gradient descent technique is given by

$$T_\Delta = -E_{var} \tag{22}$$

That is,

$$T_\Delta = \sqrt{1-\bar{\alpha}^2}\big(L(x,y)\big(M(x,y) - T(x,y)\big)\big) + \bar{\alpha}\left(\frac{\partial^2 T}{\partial x^2} + \frac{\partial^2 T}{\partial y^2}\right) = \sqrt{1-\bar{\alpha}^2}\big(L(x,y)\big(M(x,y) - T(x,y)\big)\big) + \bar{\alpha} \bigtriangledown^2 T(x,y) \tag{23}$$

Hence, T is updated as

$$T = T + \tau T_\Delta \tag{24}$$

where τ represents the step-size. The updated threshold surface, T is used to update the values of $\hat{F}(T)$ and $G(T)$. Similarly, in next iteration, these updated $\hat{F}(T)$ and $G(T)$ are used to evaluate $\bar{\alpha}$ by using Eq. (12), which is then used to update T, $\hat{F}(T)$ and $G(T)$. This iterative update of $\hat{F}(T)$ and $G(T)$ continues till it reaches predetermined number of iterations, n or satisfies the convergence condition, i.e., change in $\bar{\alpha}$ is less than a predetermined threshold, ϵ. Experimentally, n is chosen to 100 and ϵ is the smallest possible value of $\bar{\alpha}$, which is 2^{-52} in our case.

T is used to binarize M to obtain vein location V_l by

$$V_l(x,y) = \left\{\begin{array}{ll} 1 & \text{if } M(x,y) > T(x,y) \\ 0 & \text{otherwise} \end{array}\right\} \tag{25}$$

Non-uniform illumination can generate small isolated blobs or holes in V_l. These blobs are removed by standard morphological operations. Templates I_M are defined by M corresponding to the vein locations only and are given by

$$I_M = M * V_l \tag{26}$$

where $*$ represents element-wise product. This I_M depicts the veins such that vein pixels near vein endings have low intensities as compared to the vein pixels lying close to the center of the vein. Examples of T, M and I_M are shown in Fig. 4.

5.1. Numerical implementation

Basic two dimensional heat equation is

$$\frac{\partial u}{\partial t} = c\left(\frac{\partial^2 u}{\partial x^2} + \frac{\partial^2 u}{\partial y^2}\right) \tag{27}$$

where u is a function depending on x, y and t while c is a constant. The numerical solutions of such a heat equation can be given by the finite difference method [30]. It can be seen that Eq. (23) denotes a heat equation [31] where source term, S_t is given by

$$S_t = \sqrt{1-\bar{\alpha}^2}\big(L(x,y)\big(M(x,y) - T(x,y)\big)\big) \tag{28}$$

Therefore, all continuous derivatives in Eq. (23) can be replaced by the difference formula which involve the calculations at only discrete finite values. That is,

$$\left(\frac{\partial T(x,y)}{\partial x}\right)_t = T^t_{i+1,j} - T^t_{i,j} \tag{29}$$

$$\left(\frac{\partial T(x,y)}{\partial y}\right)_t = T^t_{i,j+1} - T^t_{i,j} \tag{30}$$

$$\left(\frac{\partial^2 T}{\partial x^2}\right)_t = T^t_{i+1,j} - 2T^t_{i,j} + T^t_{i-1,j} \tag{31}$$

$$\left(\frac{\partial^2 T}{\partial y^2}\right)_t = T^t_{i,j+1} - 2T^t_{i,j} + T^t_{i,j-1} \tag{32}$$

where t represents iteration number while i and j denote the pixel indices. Eq. (23) can be represented in discrete form by:

$$T^{t+1}_{i,j} = T^t_{i,j} + \tau\sqrt{1-\bar{\alpha}^2}\big(L_{i,j}\big(M_{i,j} - T^t_{i,j}\big)\big) + \tau\bar{\alpha}\big(T^t_{i+1,j} + T^t_{i-1,j} + T^t_{i,j+1} + T^t_{i,j-1} - 4T^t_{i,j}\big) \tag{33}$$

It has been shown in [32] that τ should be less than or equal to $\frac{1}{4}$. Thus, τ is equal to $\frac{1}{4}$ in this paper.

6. Vein matching

This section presents the strategy to match two vein templates. Let I^M and I^F denote the vein templates required for vein matching. For vein matching, I^M is registered with reference to I^F and overlapping vein pattern between the registered images is used to calculate the matching score.

In a registration technique, a moving image is transformed such that it is maximally similar to the fixed image. It minimizes an error function obtained from a fixed image and transformed moving image [33]. It can be noted that: (i) affine registration can handle the shear transformations produced by different finger poses; (ii) global matching performs better than local matching because local features (like minutiae and SURF descriptors [34]) can be missed or displaced due to non-uniform illumination; and (iii) one should use gray scale image during registration rather than binary image because significant useful information can be lost due to binarization. Hence, Sum of Squared Differences (SSD) on image intensities and affine transformations are used to define the error function, E, as

$$E(A) = \sum_i \big(I^F_i - A\big(I^M_i\big)\big)^2 \tag{34}$$

where i denotes pixel location and A is the affine transformation matrix which is used to register I^M with respect to I^F. Unknown parameters in matrix A are estimated by

$$\hat{A} = \arg\min_A E(A) \tag{35}$$

This can be solved by the gradient descent optimizer [35]. For initialization of A, translation parameter and angles are used to be zero. A is iteratively updated by gradient descent optimization. Let I^M_T be the transformed image of I^M which is obtained after affine registration, that is

$$I^M_T = \hat{A}\big(I^M\big) \tag{36}$$

To calculate the matching score between I^M and I^F, I^M_T and I^F are binarized to generate $\bar{I}^M_T$ and $\bar{I}^F$ by using a threshold of zero. The number of overlapping vein pixels between I^M_T and I^F, is given by

Algorithm 4 *Vein_Matching*(I^M, I^F).

Require: Two vein templates I^M and I^F
Ensure: Return S which is the matching score between I^M and I^F
1: Find affine transformation matrix, $\hat{A}$, by using gradient descent optimization and sum of squared difference cost function.
2: $I^M_T = \hat{A}(I^M)$ // Obtaining transformed image
3: Binarize I^M_T and I^F to obtain $\bar{I}^M_T$ and $\bar{I}^F$ respectively.
4: $S = \frac{\sum_x \sum_y \bar{I}^M_T(x,y) \times \bar{I}^F(x,y)}{\max(\sum_x \sum_y \bar{I}^M_T(x,y), \sum_x \sum_y \bar{I}^F(x,y))}$
5: **return** S

$$N_M = \sum_x \sum_y \bar{I}^M_T(x,y) \times \bar{I}^F(x,y) \tag{37}$$

Matching score between I^M and I^F is given by

$$S\big(I^M, I^F\big) = \frac{N_M}{\bar{T}_F} \tag{38}$$

where $\bar{T}_F$ is the maximum number of vein pixels in either $\bar{I}^M_T$ or $\bar{I}^F$. That is

$$\bar{T}_F = \max\left(\sum_x \sum_y \bar{I}^M_T(x,y), \sum_x \sum_y \bar{I}^F(x,y)\right) \tag{39}$$

Basic steps involved during vein matching are shown in Algorithm 4.

7. Experimental results

In this section, performance of the proposed system is analyzed. For this Finger Image Database (Version 1.0) [36] of PolyU has been used. It contains (i) high temporal changes due to large time gap between two sessions; (ii) large number of classes; and (iii) multiple samples per class. It consists of 3132 unconstrained finger vein images acquired from 156 subjects has been used. Among 156 subjects, there are 105 subjects who have given the data in two separate sessions while the remaining subjects have given only one session data. Average time gap between the two sessions is more than two months. Each subject has given six images of the index and middle finger of the left hand in each session, that is, total 12 images per user per session. Unconstrained acquisition system is used for data acquisition which is free from pegs or any other docking device. Further, it is a completely touch-less which avoids direct contact between sensors and finger.

Since temporal and pose variations are introduced due to large time gap between two sessions, effectiveness of the proposed system is tested by using the data from both sessions. We have used 2520 unconstrained finger vein images acquired from 105 subjects in two sessions for evaluation. Finger vein images from first session are used as training set while that of second session is used as testing set. The experimental results for various other systems in terms of equal error rate (EER) are given in Table 1 where first two columns provides result of a particular finger type and in the last column, different fingers of the same subject are considered as different classes. The proposed system has been compared with some systems proposed in [3,5] and [6]. Results are shown in the table. Also, receiver operating characteristic (ROC) curves are shown in Fig. 5. It is found that the proposed system performs better than all these systems.

The performance of various vein enhancement, vein extraction and vein matching algorithms are thoroughly analyzed in terms of EER and is shown in Table 2. For this, various combinations of vein enhancement, vein extraction and vein matching algorithms are considered to form various systems. It uses maximum curvature [6], line tracking [5], the proposed matched filtering, and the proposed multi-scale matched filtering to enhance vein; local [3], global [22] and the proposed variational based thresholding for

Table 1
Comparison with other systems in terms of EER.

	Vein enhancement algorithm	Only index	Only middle	Both index and middle
[5]	Line Tracking	13.38%	15.95%	14.26%
[6]	Maximum Curvature	12.23%	15.17%	13.78%
[3]	Gabor Filtering	3.33%	6.99%	4.91%
Proposed	**Variational Approach**	**2.98%**	**6.52%**	**4.47%**

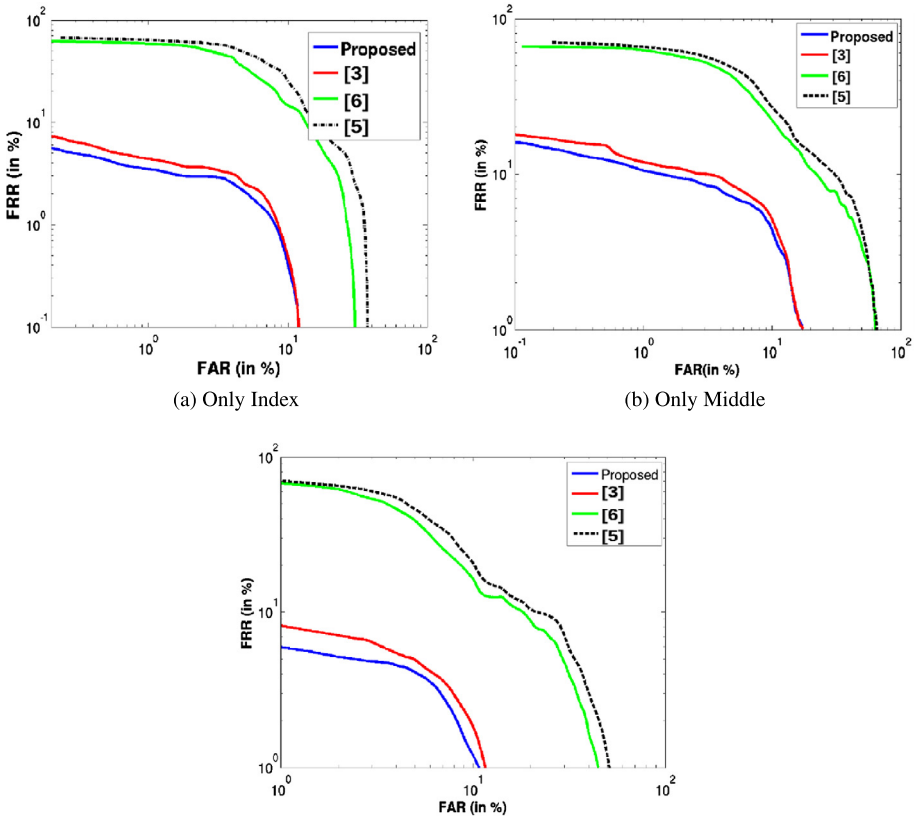

(a) Only Index (b) Only Middle

(c) Both Index and Middle

Fig. 5. ROC curves corresponding to Table 1.

Table 2
Performance evaluation of various stages in terms of EER.

Enhancement	Extraction	Matching	EER	System
Matched filter	Global	rigid	20.43%	1
		affine	20.31%	2
Matched filter	Local	rigid	11.83%	3
		affine	11.41%	4
Multi-scale matched filter	Global	rigid	18.54%	5
		affine	18.36%	6
Multi-scale matched filter	Local	rigid	9.52%	7
		affine	9.07%	8
Line tracking	Global	rigid	15.14%	9
		affine	14.26%	10
Multi-scale matched filter + Matched filter	Variational	rigid	9.22%	11
		affine	8.73%	12
Matched filter + Line tracking	Variational	rigid	6.39%	13
		affine	5.78%	14
Multi-scale matched filter + Line tracking	Variational	rigid	4.73%	15
		affine	**4.47%**	**16**

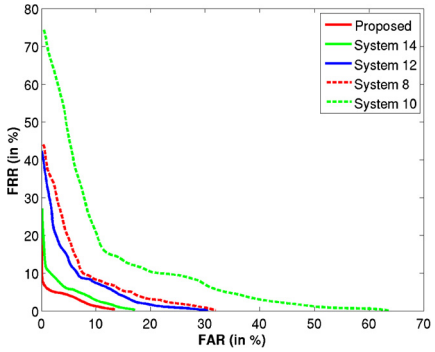

Fig. 6. ROC curves for some systems described in Table 2.

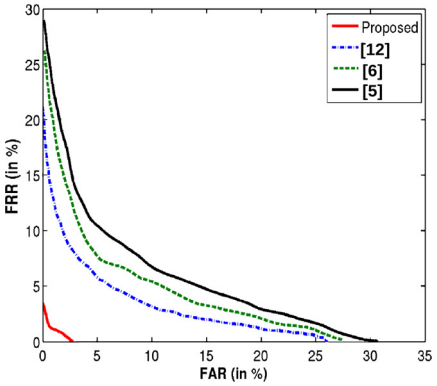

Fig. 7. ROC curve for some systems employing first session data.

vein extraction; and rigid [3] and the proposed affine based registration for vein matching. Description of each system is shown in Table 2. Corresponding ROC curves are shown in Fig. 6. We have considered different fingers of the same subject as different classes. Some observations derived from Table 2 are:

- The proposed system enhances the vein pattern by applying multi-scale matched filter along with local adaptive thresholding. It shows better performance in comparison to other systems which uses matched filter, maximum curvature or line tracking. This is because of the fact that: (i) multi-scale matched filter uses matched filter at multiple resolutions to remove noise and extract variable width veins; and (ii) multi-scale matched filter uses vein shapes more effectively than line tracking and maximum curvature.
- Two vein enhanced images are used for vein pattern extraction in Systems 11–16 while in Systems 1–10 veins are extracted by using a single vein enhanced image. It can be seen that Systems 11–16 have better performance than Systems 1–10. It can be inferred that better vein extraction can be expected if two enhanced vein images are used for vein extraction. This may be due to the use of two complementary representations and the use of variational approach.
- Systems 11 and 12 have poor performance than Systems 13–16. This can be due to the fact that multi-scale matched filter is obtained by using matched filters. Hence, vein enhanced images in Systems 13 and 14 do not have much complementary information.
- Systems 13 and 14 have poor performance than Systems 15 and 16 respectively. This is because multi-scale matched filter represents the vein pattern much more accurately than matched filter. It emphasizes that the performance of the proposed system is dependent on the individual vein representation.
- Local thresholding based vein extraction gives better EER than global thresholding based vein extraction which fails mainly due to non-uniform illumination. In addition, it is not useful for the line tracking based enhanced images where the background areas contain significant variations [5]. If it is used for line tracking based enhanced images, then an EER of 47.38% and 46.91% are obtained for rigid and affine registration based vein matching respectively.
- Systems based on affine registration always give better EER than its corresponding rigid registration based system. It indicates that changes in finger poses can be effectively handled by affine registration as compared to rigid registration.
- The proposed system (System 16) performs better than various other system.

In addition, the performance of the proposed system is further analyzed by using different testing strategy used in [12]. It employs data of 156 subjects from the first session. Hence, total 1872 images obtained from 312 different classes are considered. There is a large difference between numbers of intra-class and inter-class matching which is reduced by (i) considering all six images per finger during intra-class matching; and (ii) considering only first two images per finger during inter-class matching. Thus, there are 4680 intra-class matchings and 194,064 inter-class matchings used during testing [12]. With such a data set and testing strategy, EERs of systems proposed in [5,6] and [12] are found to be 8.13%, 6.87% and 5.53% respectively while EER of the proposed system is 1.11%. The ROC curves for these systems are shown in Fig. 7. Therefore, it can be inferred that the proposed system performs better. It is mainly due to the effective vein extraction and affine registration based matching which handles efficiently the pose variation. It has been observed that in some cases, finger area is not appropriately acquired due to heavy illumination which results in missing of genuine vein pattern. Due to this, the performance of the system suffers because less genuine vein pattern is available. It is applicable to all well known vein pattern based authentication systems.

At IIT Kanpur [37], we are developing various unimodal biometric systems. Among them, palm print, ear, iris, face, fingerprint, palm dorsal systems are worth to mention. Some useful properties of these systems are:

1. **Palm print based system:** This system [38] uses a high quality camera for palm print image acquisition. The images are found to contain good quality, uniform illumination, less noise and abundant texture. Area of palm print is localized from the acquired image using the domain knowledge of hand. It is divided into non-overlapping blocks. Texture of each block is enhanced by applying histogram equalization. Texture in a block is summed up in horizontal and vertical directions to obtain horizontal and vertical profile respectively. Phase of a profile is obtained using Fourier transform and used as a feature. Corresponding phase profiles of each block between two palm prints are matched to obtain the matching score using hamming distance. Eventually, matching scores are fused using score level fusion. PolyU dataset [39] having 7752 images acquired from 386 different palms is used for performance evaluation. It has shown the performance with an EER of 0.02%.
2. **Ear based system:** Images acquired in the system [40] are also rich is texture and are of good quality. Three image enhancement techniques, viz., adaptive histogram equalization, non-local means filter and steerable filter are applied to enhance the contrast, remove the noise and remove the artifacts of illumination respectively. Local features of each enhanced image are extracted using speedup robust features that can handle the artifacts of occlusion and are found to invariant against pose, scale and illumination [41]. It is observed that some features may be absent in an enhanced image due to occlusion.

Table 3
Comparative studies.

Modality	System	Dataset		Feature extraction	Feature matching	EER (%)
		Classes	Total			
Palm print	[38]	386	7752	Horizontal and vertical profile	Phase matching	0.02
Ear	[40]	114	464	Speedup robust features (SURF)	Nearest neighbor matching	3.8
Iris	[43]	819	16,212	Corners	Lucas–Kanade	1.29
Face	[44]	200	400	Manual annotation	Self organizing map	14.39
Fingerprint	[33]	1200	7200	NIST [45]	NIST [45]	21
Palm dorsal vein	[46]	990	4950	Thresholding + minutiae detection	Minutiae matching	0.79
Finger veins	Proposed	312	3132	Variational fusion + Thresholding	Registration based matching	4.47

Hence, features from various images of a user are fused to achieve better performance. For each user, three types of local features based on the enhancement type, are stored in the database. Local features corresponding to an enhanced image are matched using the nearest neighbor classifier. Eventually, matching scores are fused using score level fusion. The system has achieved an EER of 3.8% on UND-E database [42] consisting of 464 images acquired from 114 users.

3. **Iris based system:** An iris image consists of inner and outer boundaries. In the system [43], inner boundary is detected by applying the threshold algorithm, edge detection filters and Hough transform, while outer boundary is detected by applying circular integral and differential operators. Detected iris is mapped onto a fixed size image for normalization. Local texture enhancement, contrast limited adaptive histogram equalization and Weiner filtering are applied to the mapped image to remove illumination artifacts and noise while enhancing the contrast. Corners are detected from the enhanced image. Optical flow matching based on Lucas–Kanade tracking is used for matching the corners. The system has achieved an EER of 1.29% on Lamp database that consists of 16,212 images acquired from 819 users.
4. **Face based system:** Various face based authentication systems have been developed in the IITK, each of which focuses on different type of challenges such as effect of illumination, expression, pose variations, bad quality and occlusion. The system proposed in [44] is an expression invariant system. Using the manually annotated eye locations and domain knowledge of facial geometry, face is localized and cluttered background is removed. It has been observed that one should avoid the matching of mouth area for expression invariant face recognition system because lots of variations are introduced near mouth regions when facial expression is changed. In this system, an area near mouth region is darkened to avoid the matching. Self organizing map is used for dimensionality reduction. Eventually, nearest neighbor classifier is used for authentication. The system has been evaluated using FERET Database containing 400 images acquired from 200 individuals. It has achieved an EER of 14.39%.
5. **Fingerprint based system:** The fingerprint system [33] uses the NIST feature extractor, Mindtct, to extract the fingerprint minutiae and NIST matcher, bozorth, for minutiae matching [45]. The system [33] gives accurate results for good quality fingerprints but fails for poor quality fingerprint images. The performance of the system is assessed using a database consisting of 7200 images acquired from 1200 classes. It is to be noted that the database is acquired from the rural people who are involved in significant manual work and belong to different age groups. Hence, smoothen ridge-valley structure, creases, scars, wound and dirt are common on the fingertips of the users. In addition, image acquisition is performed in an unconstrained environment. The database consists of bad quality fingerprints [23]. The system has shown an EER of 21%.
6. **Palm dorsal based system:** Vein pattern is considered to be the most promising biometric trait because apart from the advantages of biometric traits like uniqueness, universality and permanence, it also (i) assures liveness; (ii) is hard to forge as it lies in the skin; (iii) is difficult to spoof; and (iv) has low failure to enroll. The vein pattern based authentication system proposed in [46] requires palm dorsal vein pattern. A setup has been designed in this system which restrains pose variation and visible light but it maintains uniform illumination and high contrast between veins and neighboring pixels. The palm dorsal area is localized from the acquired image using active contour. Due to large intensity differences in the vein and non-vein pixels, vein pattern is extracted using a global threshold algorithm. Minutiae like ridge termination and ridge ending are extracted from the vein pattern. Minutiae matching is carried out using the Euclidean distance for authentication. The proposed system has been evaluated on IITK database containing 4950 images acquired from 990 classes. It has reported an EER of 0.79%.

Epitome of these systems is given in Table 3. Vein enhancement algorithms proposed in this paper are based on local and global properties of vein pattern. It helps to handle the problems like non-uniform illumination, low local contrast and noise. Extracted veins are fused by a variational approach for accurate vein extraction. Further, affine registration based matching is used to handle the problem of pose variation. A highly challenging database containing large temporal changes has been used for experimental evaluation to justify its applicability. The proposed system has been evaluated on Finger Image Database (Version 1.0) [36] containing 3132 images acquired from 312 classes. It has reported an EER of 4.47%.

8. Conclusion

This paper has proposed an efficient finger vein based personal authentication system. For vein enhancement, a multi-scale matched filter has been used to deal with the noise occurred due to non-uniform illumination, low local contrast, hair and skin texture. It has used local neighborhood characteristics. Veins have also been enhanced by using global characteristics. Both the enhanced vein images obtained with the help of local and global characteristics have been fused to obtain the vein pattern. It has been observed that the problem of geometric deformation can decrease the performance of vein matching. Any geometrical deformation can be introduced due to different finger poses, contact-less and unconstrained image acquisition. To handle such type of deformation, affine registration has been used during vein matching. A publicly available database containing 3132 unconstrained finger vein images from 156 subjects has been used for performance evaluation. Experimental results have indicated that the proposed system performs better than the various existing systems.

Acknowledgments

The authors are grateful towards anonymous reviewers whose comments have helped us to improve the quality of the paper. This work is partially supported by the Department of Information Technology (DIT), Government of India.

References

[1] B. Huang, Y. Dai, R. Li, D. Tang, W. Li, Finger-vein authentication based on wide line detector and pattern normalization, in: International Conference on Pattern Recognition, IEEE, 2010, pp. 1269–1272.
[2] J. Yang, X. Li, Efficient finger vein localization and recognition, in: International Conference on Pattern Recognition, IEEE, 2010, pp. 1148–1151.
[3] A. Kumar, Y. Zhou, Human identification using finger images, IEEE Trans. Image Process. 21 (4) (2012) 2228–2244.
[4] Z. Zhang, S. Ma, X. Han, Multiscale feature extraction of finger-vein patterns based on curvelets and local interconnection structure neural network, in: International Conference on Pattern Recognition, IEEE, 2006, pp. 145–148.
[5] N. Miura, A. Nagasaka, T. Miyatake, Feature extraction of finger-vein patterns based on repeated line tracking and its application to personal identification, Mach. Vis. Appl. 15 (4) (2004) 194–203.
[6] N. Miura, A. Nagasaka, T. Miyatake, Extraction of finger-vein patterns using maximum curvature points in image profiles, IEICE Trans. Inf. Syst. 90 (8) (2007) 1185–1194.
[7] J. Yang, Y. Shi, Finger-vein ROI localization and vein ridge enhancement, Pattern Recognit. Lett. 33 (12) (2012) 1569–1579.
[8] J. Yang, Y. Shi, Towards finger-vein image restoration and enhancement for finger-vein recognition, Inf. Sci. 268 (2014) 33–52.
[9] D. Hartung, M.A. Olsen, H. Xu, C. Busch, Spectral minutiae for vein pattern recognition, in: International Joint Conference on Biometrics, IEEE, 2011, pp. 1–7.
[10] B.A. Rosdi, C.W. Shing, S.A. Suandi, Finger vein recognition using local line binary pattern, Sensors 11 (12) (2011) 11357–11371.
[11] J. Peng, N. Wang, A.A.A. El-Latif, Q. Li, X. Niu, Finger-vein verification using Gabor filter and sift feature matching, in: International Conference on Intelligent Information Hiding and Multimedia Signal Processing, IEEE, 2012, pp. 45–48.
[12] L. Yang, G. Yang, Y. Yin, X. X, Exploring soft biometric trait with finger vein recognition, Neurocomputing 135 (2014) 218–228.
[13] J. Yang, Y. Shi, J. Yang, L. Jiang, A novel finger-vein recognition method with feature combination, in: International Conference on Image Processing, IEEE, 2009, pp. 2709–2712.
[14] Z. Liu, Y. Yin, H. Wang, S. Song, Q. Li, Finger vein recognition with manifold learning, J. Netw. Comput. Appl. 33 (3) (2010) 275–282.
[15] K.R. Park, Finger vein recognition by combining global and local features based on SVM, Comput. Inform. 30 (2) (2012) 295–309.
[16] B.J. Kang, K.R. Park, Multimodal biometric authentication based on the fusion of finger vein and finger geometry, Opt. Eng. 48 (9) (2009) 090501.
[17] A. Pflug, D. Hartung, C. Busch, Feature extraction from vein images using spatial information and chain codes, Inf. Secur. Tech. Rep. 17 (1) (2012) 26–35.
[18] L. Yang, G. Yang, Y. Yin, R. Xiao, Sliding window-based region of interest extraction for finger vein images, Sensors 13 (3) (2013) 3799–3815.
[19] J.-D. Wu, S.-H. Ye, Driver identification using finger-vein patterns with radon transform and neural network, Expert Syst. Appl. 36 (3) (2009) 5793–5799.
[20] N. Mahri, S. Suandi, B.A. Rosdi, Finger vein recognition algorithm using phase only correlation, in: International Workshop on Emerging Techniques and Challenges for Hand-Based Biometrics, IEEE, 2010, pp. 1–6.
[21] W. Yang, X. Huang, F. Zhou, Q. Liao, Comparative competitive coding for personal identification by using finger vein and finger dorsal texture fusion, Inf. Sci. 268 (2014) 20–32.
[22] N. Otsu, A threshold selection method from gray-level histograms, Automatica 11 (285–296) (1975) 23–27.
[23] P. Gupta, P. Gupta, Slap fingerprint segmentation, in: International Conference on Biometrics: Theory, Applications and Systems, IEEE, 2012, pp. 189–194.
[24] P. Gupta, P. Gupta, An efficient slap fingerprint segmentation and hand classification algorithm, Neurocomputing 142 (2014) 464–477, http://dx.doi.org/10.1016/j.neucom.2014.03.049.
[25] S. Chaudhuri, S. Chatterjee, N. Katz, M. Nelson, M. Goldbaum, Detection of blood vessels in retinal images using two-dimensional matched filters, IEEE Trans. Med. Imaging 8 (3) (1989) 263–269.
[26] T. Lindeberg, Scale-Space Theory in Computer Vision, Springer, 1993.
[27] W. Song, T. Kim, H.C. Kim, J.H. Choi, H.-J. Kong, S.-R. Lee, A finger-vein verification system using mean curvature, Pattern Recognit. Lett. 32 (11) (2011) 1541–1547.
[28] B.N. Saha, N. Ray, Image thresholding by variational minimax optimization, Pattern Recognit. 42 (5) (2009) 843–856.
[29] A. Pascual-Iserte, D.P. Palomar, A.I. Pérez-Neira, M.Á. Lagunas, A robust maximin approach for MIMO communications with imperfect channel state information based on convex optimization, IEEE Trans. Signal Process. 54 (1) (2006) 346–360.
[30] G.W. Recktenwald, Finite-difference approximations to the heat equation, class notes, http://www.f.kth.se/~jjalap/numme/FDheat.pdf, 2004.
[31] P. DuChateau, D. Zachmann, Applied Partial Differential Equations, Courier Dover Publications, 2012.
[32] G. Evans, J. Blackledge, P. Yardley, Numerical Methods for Partial Differential Equations, 2005.
[33] P. Gupta, P. Gupta, A dynamic slap fingerprint based verification system, in: International Conference on Intelligent Computing, Springer, 2014, pp. 812–818.
[34] M. Pan, W. Kang, Palm vein recognition based on three local invariant feature extraction algorithms, in: Biometric Recognition, Springer, 2011, pp. 116–124.
[35] D.P. Shamonin, E.E. Bron, B.P. Lelieveldt, M. Smits, S. Klein, M. Staring, A.D.N. Initiative, et al., Fast parallel image registration on CPU and GPU for diagnostic classification of Alzheimer's disease, Frontiers in Neuroinformatics 7 (50) (2013) 1–15.
[36] The Hong Kong Polytechnic University finger image database (version 1.0), http://www4.comp.polyu.edu.hk/~csajaykr/fvdatabase.htm.
[37] IITK Biometrics Lab, http://www.cse.iitk.ac.in/users/biometrics/.
[38] G. Badrinath, P. Gupta, Palmprint based recognition system using phase-difference information, Future Gener. Comput. Syst. 28 (1) (2012) 287–305.
[39] The PolyU palmprint database, http://www.comp.polyu.edu.hk/~biometrics.
[40] S. Prakash, P. Gupta, An efficient ear recognition technique invariant to illumination and pose, Telecommun. Syst. 52 (3) (2013) 1435–1448.
[41] H. Bay, T. Tuytelaars, L. Van Gool, Surf: speeded up robust features, in: Computer Vision, ECCV 2006, Springer, 2006, pp. 404–417.
[42] University of Notre Dame ear database, collection e, http://www.nd.edu/cvrl/CVRL/DataSets.html.
[43] A. Nigam, P. Gupta, Iris recognition using consistent corner optical flow, in: Computer Vision, ACCV 2012, Springer, 2013, pp. 358–369.
[44] R. Varma, S. Gupta, P. Gupta, Face recognition system invariant to expression, in: Intelligent Computing Theory, Springer, 2014, pp. 299–307.
[45] C.I. Watson, M.D. Garris, E. Tabassi, C.L. Wilson, R.M. McCabe, S. Janet, Users guide to NIST fingerprint image software 2 (NFIS2), National Institute of Standards and Technology.
[46] M. Soni, P. Gupta, A robust vein pattern-based recognition system, J. Comput. 7 (11) (2012) 2711–2718.

Puneet Gupta is a research scholar in the Department of Computer Science and Engineering, Indian Institute of Technology Kanpur, India. His area of research includes Biometrics, Image Processing and Computer Vision.

Phalguni Gupta is the director of National Institute of Technical Teachers Training and Research, Kolkata. He is also associated with Department of Computer Science and Engineering, Indian Institute of Technology Kanpur, India. He received his PhD degree in computer science and engineering from Indian Institute of Technology Kharagpur, India, in 1986. Prior to joining IIT Kanpur, he was with the Image Processing and Data Product Group of the Space Applications Center (ISRO), Ahmedabad, India (1983–1987) and was responsible for correcting image data received from Indian Remote Sensing Satellite. His research interest includes sequential algorithms, parallel algorithms, online algorithms, image processing, biometrics, identity and infrastructure management. Currently, he is responsible for several research projects in the area of image processing, biometrics and parallel processing. He has published over 250 peer-reviewed journals and conference papers. He is also an author of 2 books and 14 book chapters. He is a member of the Association Computing Machinery (ACM) and recipient of 2007 IBM Faculty Award.